ACCSCIENCE PUBLISHING

Eurasian Journal of Medicine and Oncology

ORIGINAL RESEARCH ARTICLE

Targeting STAT3 enhances glioblastoma therapeutic sensitivity through valproic acid-mediated regulation of the tumor microenvironment

Leina Li, Moli Wu, Xu Zheng, and Jia Liu*

Liaoning Laboratory of Cancer Genomics and Epigenomics, College of Basic Medical Sciences, Dalian Medical University, Dalian, Liaoning, China

Abstract

Introduction: Glioblastoma (GBM) is a highly malignant tumor of the nervous system, posing serious threats to patient survival and quality of life. However, current treatment options remain limited in both availability and effectiveness.

Objective: This study analyzes the gene expression data related to GBM to support the development of improved therapeutic strategies.

Methods: Two gene expression datasets were selected for statistical analysis. Differentially expressed genes (DEGs) related to GBM were screened based on predefined criteria. Enrichment analysis was performed to explore the biological processes and pathways involved. A protein-protein interaction (PPI) network was constructed to identify central genes, which were further analyzed for expression patterns and their potential roles in GBM pathology.

Results: A total of 1,151 overlapping DEGs were identified. Enrichment analysis revealed their involvement in several key biological processes and pathways. From the PPI network, central genes, including signal transducer and activator of transcription 3 (STAT3), CAML1, clathrin assembly lymphoid myeloid 2, and protein kinase CAMP-activated catalytic subunit beta were identified as playing crucial roles in GBM development. Immune cell subtype analysis indicated interactions between these genes and the tumor microenvironment. The diagnostic value highlighted STAT3 as a potential biomarker for GBM. *In vivo* experiments confirmed that gene expression patterns were consistent with database predictions. Molecular docking analysis identified valproic acid as a promising therapeutic candidate, targeting five central genes. *In vitro* studies demonstrated that valproic acid effectively induced GBM cell death and modulated the expression of these genes, with high safety observed.

Conclusion: Identifying DEGs and central genes is essential in understanding GBM pathology. This study establishes STAT3 as a diagnostic marker and highlights valproic acid as a potential multi-target therapeutic agent. These findings lay the groundwork for more effective and targeted treatment strategies for GBM.

Keywords: Glioblastoma; Signal transducer and activator of transcription 3; Differentially expressed genes; Valproic acid

***Corresponding author:**
Jia Liu
(jialiudl@dmu.edu.cn)

Citation: Li L, Wu M, Zheng X, Liu J. Targeting STAT3 enhances glioblastoma therapeutic sensitivity through valproic acid-mediated regulation of the tumor microenvironment. *Eurasian J Med Oncol*. 2025;9(4):209-227. doi: 10.36922/EJMO025140076

Received: March 31, 2025

Revised: April 29, 2025

Accepted: May 9, 2025

Published online: June 23, 2025

1. Introduction

Glioblastoma (GBM) is a highly invasive primary brain tumor.[1] That poses a serious threat to patient health. Although numerous studies have investigated treatment strategies for GBM, significant progress remains limited, and the prognosis of most patients is still poor.[2] Currently, the standard treatment for GBM includes postoperative radiotherapy and chemotherapy, with temozolomide being a commonly used chemotherapeutic agent.[3-5] However, these treatments do not significantly improve patients' quality of life and offer limited efficacy. Therefore, there is an urgent need for in-depth research into novel therapeutic strategies, which remains a key focus in the field. Bioinformatics is widely applied in the study of disease-related genes and can support the development of targeted therapies by analyzing large-scale genomic and transcriptomic data.[6] Using bioinformatics, researchers can identify molecular characteristics and therapeutic targets across various cancers.[7,8] This study applies bioinformatics methods to analyze genetic datasets in order to identify genes closely associated with GBM and to discover targeted therapeutic drugs, providing a foundation for more effective treatment.

The molecular mechanisms underlying GBM can be elucidated by identifying relevant hub genes. These genes are of great significance in improving the accuracy of GBM treatment and supporting the development of targeted drugs. In this study, gene expression datasets related to GBM were first downloaded, and transcriptome profiles of normal and GBM samples were compared using bioinformatics methods to identify differentially expressed genes (DEGs) closely associated with GBM. To meet the requirements of targeted therapy,[9] it is necessary to identify potential candidate drugs for GBM. However, based on extensive clinical experience, temozolomide-related drugs have shown low specificity and are prone to causing side effects, which significantly limits their clinical application. Therefore, this study searched drug databases to identify compounds that are cytotoxic to GBM cells and capable of inducing apoptosis.[10]

The innovation of this study lies in the integration of bioinformatics and computational drug screening to identify DEGs and candidate drugs closely related to GBM. The findings provide valuable insights into the molecular mechanisms of the disease and offer theoretical guidance for targeted therapy. The significance of this study is twofold. First, it contributes to a deeper understanding of GBM pathogenesis and offers a reference for identifying relevant therapeutic targets. Based on the identified central genes, more precise and personalized treatment strategies can be developed to support clinical interventions. Second, the discovery of targeted drugs for GBM may improve patient prognosis and reduce adverse side effects. Molecular biology analyses enable the design of therapies that selectively attack cancer cells while sparing normal cells, thereby reducing off-target toxicity and enhancing therapeutic outcomes.

In summary, this study identified key genes and candidate therapeutic compounds for GBM through gene database analysis, clarified the relevant therapeutic targets, and provided guidance for the development of efficient diagnostic tools and targeted treatments.

2. Materials and methods

2.1. Database selection

A search was conducted in the gene expression omnibus (GEO) database to identify two microarray gene expression datasets closely related to GBM: GSE151352 and GSE184643. The former includes data from 12 GBM patients who underwent surgical treatment, analyzed using RNA sequencing to determine matched pairs of healthy and cancer samples, thereby supporting subsequent differential analysis.[11] The latter dataset primarily includes transcriptome sequencing data of these patient sample pairs and is mainly used to determine the biological characteristics of GBM and inform targeted therapies.

2.2. Analysis of DEGs

After obtaining the two datasets, the data were normalized using the LIMMA package in R, followed by differential analysis using the DESeq2 tool. The criteria for identifying DEGs were $|\log_2(FC)| > 1$, $p<0.05$, resulting in a total of 1,151 DEGs. Overlapping DEGs were also identified.[12]

2.3. Enrichment analysis of DEGs

The Kyoto Encyclopedia of Genes and Genomes (KEGG)[13] and gene ontology (GO)[14] databases were utilized to perform GO enrichment and KEGG pathway enrichment analyses on the merged set of 1,151 DEGs from the two GEO datasets.[15,16] The top 20 pathways, ranked by GO and KEGG results, were selected for analysis. Enriched pathways were identified based on a false discovery rate of <0.05.

2.4. Construction of protein-protein interaction (PPI) network

To integrate high-throughput expression data and other molecular features into a biological interaction network, a PPI network of the 1,151 merged DEGs was constructed using the STRING database and visualized with Cytoscape.[17]

2.5. Discovery of hub genes

To study the core gene network, the CytoHubb plugin in Cytoscape software was used. It contains various tools to

identify key nodes and their connections with other genes in a biological network. Different algorithms (closeness centrality, radiality, and stress) were employed to identify the top 10 hub genes. The generated network was color-coded based on the correlation of hub nodes, with red representing the highest scores and yellow the lowest.[18,19] As all three algorithms yielded the same top 10 hub genes, these 10 genes were selected as candidate hub genes for subsequent research. The expression of these central genes was then analyzed to obtain expression data from the two databases, followed by *t*-tests to determine gene expression differences between sample pairs.[20] Five significantly different genes were ultimately identified and designated as the central genes, providing support for subsequent targeted analysis.

2.6. Analysis of immune infiltration in GBM

To determine the infiltration levels of various immune cell types in GBM, the CIBERSORT algorithm was used to assess the immune infiltration landscape and quantify the infiltration levels of different immune cell types.[21] Correlation analysis using the ggplot2 package was conducted to explore the relationships between various immune cells and the central genes.

2.7. Identification of diagnostic genes

A receiver operating characteristic (ROC) curve was established, and the pROC package was used to calculate the area under the curve (AUC), which was then used to evaluate and rank the predictive performance of key genes.[22] Based on ROC curve changes between sample pairs, diagnostic genes with high diagnostic values were identified to support improvements in the diagnostic accuracy of this disease.

2.8. Prediction of potential therapeutic drugs

This study analyzed the drug signatures database (DSigDB)[23] to identify potential targeted therapeutic drugs. Currently, valproic acid has received widespread attention for the treatment of GBM. To prepare the ligand, hydrogen atoms were added to the system to optimize and adjust its geometry.[24] The Protein Data Bank library was searched to obtain the crystal structures of target proteins corresponding to the five key genes. Water molecules and heteroatoms were then removed to obtain protein structures that met the docking requirements. For the molecular docking study, AutoDock Vina software[25] was used to calculate the corresponding molecular docking strength. The results were visualized using PyMOL software to generate three-dimensional docking maps, which intuitively reflect the predicted binding mode of valproic acid at each target protein binding site.[26]

2.9. Molecular docking

The chemical structure data of sodium valproate were obtained from a database and converted into a compatible format.[27] Hydrogen atoms were added to the system to optimize the shape of the ligand and improve molecular docking performance. The crystal structures of the target proteins corresponding to the five central genes were obtained from a protein database. Water molecules and heteroatoms were removed to yield protein structures suitable for docking. Docking analysis was conducted using AutoDock Vina software.[28] Visualization and conversion of simulation results were performed using software tools to obtain a three-dimensional docking diagram. Based on these graphical results, the predicted binding mode of sodium valproate at each target protein binding site was determined.

2.10. Animal model

Sprague–Dawley rats (5 – 6 weeks old, 200 ± 20 g, $N = 6$) were obtained from the Liaoning Laboratory of Cancer Genomics and Epigenomics, College of Basic Medical Sciences, Dalian Medical University. The rats were housed in a controlled environment under pathogen-free conditions. To establish the orthotopic GBM model, 1×10^6 RG2 cells (in a volume of 10 μL) were stereotactically injected into the caudate putamen region of the rat brain. Subsequently, the rats received a 2-day course of analgesics and antibiotics.[29,30] All animal experiments were conducted under anesthesia, and every effort was made to minimize discomfort or suffering. All procedures involving experimental animals strictly adhered to the National Institutes of Health Guidelines.[31]

2.11. Quantitative real-time polymerase chain reaction (PCR)

Total RNA was extracted from normal brain and GBM tissues of rats using the TRIzol reagent. The isolated RNA was then reverse transcribed into complementary DNA utilizing the PrimeScript RT kit with gDNA Eraser.[32] To determine gene expression levels, a quantitative real-time PCR was conducted using SYBR1 Premix Ex Taq II.[33] Relative gene levels were calculated using the $2^{-\Delta\Delta Cq}$ method. The data represent the average of at least three independent experiments.

2.12. Cell culture

LN229 and LN18 cells were cultured in a medium containing 10% fetal bovine serum and 1% penicillin/streptomycin. During the cultivation process, the medium was changed every 24 h to ensure normal cell growth. A specified dose of valproic acid was added to stimulate the cells at passages 3 – 8,[34] and the cell status was observed and analyzed.

2.13. Cell proliferation assays

LN229 and LN18 cells were inoculated into a 96-well plate and incubated for 1 day. A specific dose of valproic acid was then added to treat the cells for 24 h. The following day, their proliferation rate was assessed using the cell counting kit-8 (CCK8) method.[35] After incubation, absorbance was measured at a wavelength of 405 nm, and the experiment was repeated 3 times under identical conditions to minimize experimental errors.

2.14. Microscopy observation

LN229 and LN18 cells were seeded in six-well plates. After 24 h of adhesion, the cells were treated with 10 mM valproic acid for 24 h. The next day, the cells were washed with phosphate-buffered saline and observed under a microscope. Corresponding micrographs were collected, and morphological changes of the cells were analyzed using Image J software (NIH, USA).

2.15. Scratch assay

LN229 and LN18 cells were seeded in six-well plates. Once the cells reached sufficient confluence, a scratch was made at the center of each well. The wells were gently washed with phosphate-buffered saline to remove any detached cells.[36] Subsequently, a fresh medium containing 10 mM of valproic acid was added to the wells. The plates were incubated for 24 h. Images of the scratched areas were captured at regular intervals using a microscope (Nikon, Japan). The width of the scratch was measured using image analysis software (Image J, NIH, USA) to assess the migration ability of the cells.

2.16. Western blot

Total protein was extracted from LN229 and LN18 cells treated with 10 mM of valproic acid for 24 h using radioimmunoprecipitation assay lysis buffer, and protein concentrations were determined using a bicinchoninic acid assay kit. Western blot analysis was performed to assess protein expression levels. For this purpose, equal amounts (30 μg) of protein samples were separated by sodium dodecyl sulfate-polyacrylamide gel electrophoresis using 10% and 15% gels. The separated proteins were then transferred onto polyvinylidene fluoride membranes (Millipore, USA).[37] To minimize nonspecific interactions and ensure proper binding, the membranes were blocked with 5% skimmed milk at room temperature for 1 h. Next, the membranes were incubated overnight at 4°C with the respective primary antibodies. The specific antibodies used were: signal transducer and activator of transcription 3 (STAT3; 1:1000; 9139T, Cell Signaling Technology, USA), clathrin assembly lymphoid myeloid (CALM; 1:1000; PA5-82661, ThermoFisher, USA), synaptosomal-associated protein (SNAP25, 25kDa; 1:1000; 5308T, Cell Signaling Technology, USA), protein kinase CAMP-activated catalytic subunit beta (PRKACB; 1:1000; 12232-1-AP, Proteintech, USA), and glyceraldehyde 3-phosphate dehydrogenase (GAPDH) (GAPDH; 60004-1-Ig., Proteintech, USA).

2.17. Statistical analyses

All data were analyzed using GraphPad Prism 8 (GraphPad Software Inc., CA, USA). Continuous variables are presented as mean ± standard deviation. Statistical differences between two groups were determined using the *t*-test, while differences among multiple groups were assessed using analysis of variance followed by the Bonferroni test for pairwise group comparisons.

3. Results

3.1. Identification of overlapping DEGs in GSE151352 and GSE184643 datasets

This study integrated two independent datasets (GSE151352 and GSE184643). The GSE151352 dataset comprises RNA-seq data derived from fresh paired normal and tumor tissue samples obtained from 12 surgical GBM patients, with sample groups clearly stratified based on pathological diagnosis. GSE184643 represents transcriptomic data from an independent GBM cohort. As shown in Figure 1A and B, in the GSE151352 dataset, there were a total of 1,625 downregulated genes, 11,332 genes with no significant change, and 839 upregulated genes. In the GSE184643 dataset, there were 1,909 downregulated genes, 16,019 genes with no significant change, and 1,635 upregulated genes. The heatmaps in Figure 1C and D display the expression patterns of the top 20 DEGs in both datasets. Subsequently, we identified 1,151 overlapping genes from the DEGs in GSE151352 and GSE184643 for further analysis (Figure 1E).

3.2. Functional enrichment analysis of overlapping DEGs

To further understand the roles of DEGs, we conducted a functional enrichment analysis. KEGG pathway analysis was performed on the 1,151 overlapping DEGs to identify significantly associated biological pathways. The results showed that these genes were significantly enriched in the adrenergic pathway, cell cycle, and mitogen-activated protein kinase (MAPK) pathway (Figure 2A). GO biological process enrichment analysis revealed that these genes were mainly involved in synaptic neurotransmitter transport and cell communication (Figure 2B). In the GO cellular component, the proteins

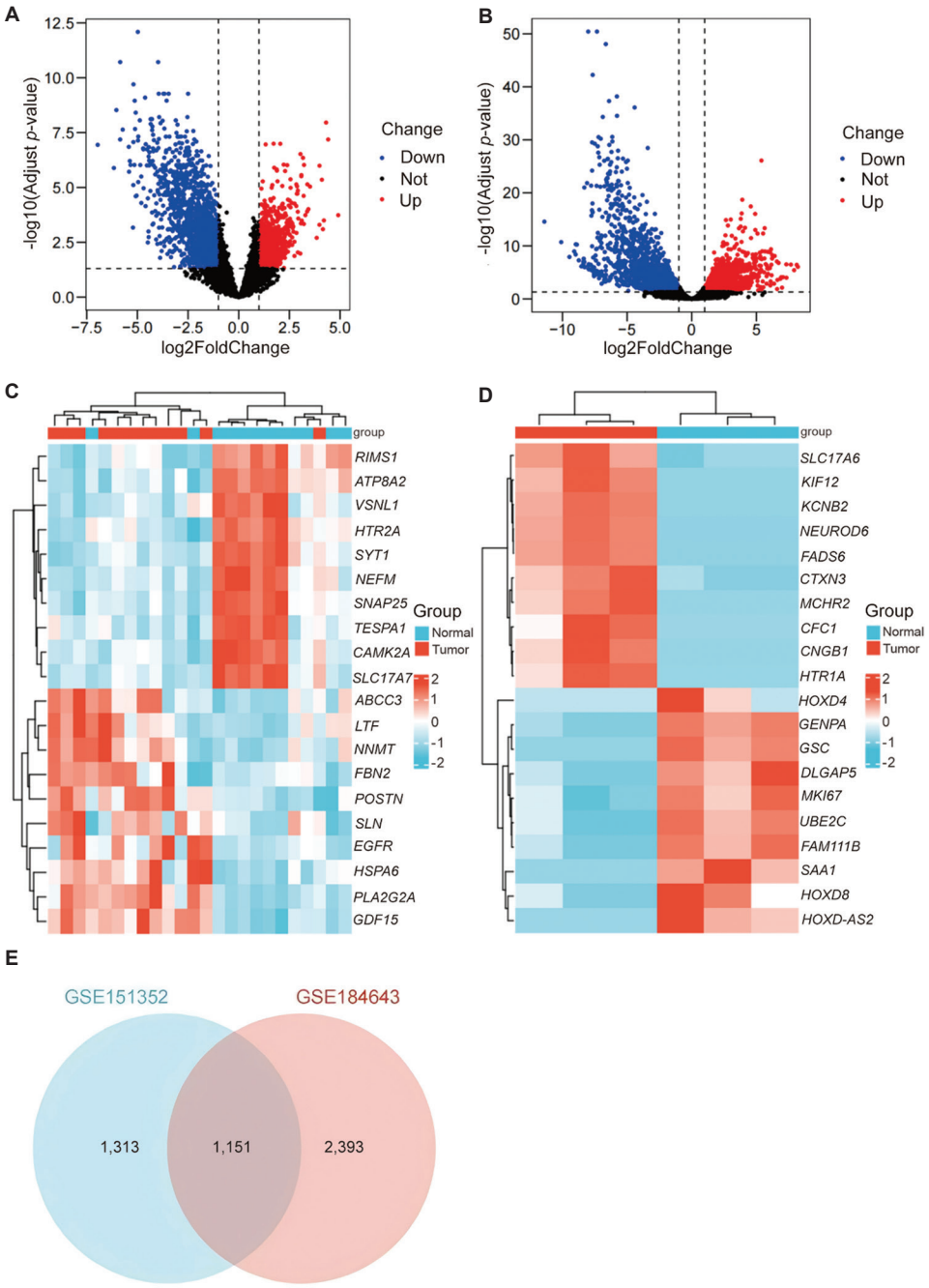

Figure 1. Differentially expressed genes (DEGs) in GSE151352 and GSE184643 datasets. Volcano plots of DEGs in (A) GSE151352 and (B) GSE184643 datasets. Red represents upregulated genes; blue represents downregulated genes. Heatmaps of the top 20 DEGs with the most significant expression changes in (C) GSE151352 and (D) GSE184643 datasets. (E) Overlapping DEGs identified from both gene expression omnibus datasets.

encoded by these genes were predominantly enriched in neurons and synapses (Figure 2C). Finally, GO molecular function (GO-MF) analysis indicated that the 1,151 overlapping DEGs were associated with cell cytoskeleton binding, kinase binding, and nucleotide binding (Figure 2D).

3.3. Identification of consistently expressed hub genes in GBM via PPI network analysis and expression validation

A PPI network of the 1,151 overlapping genes was established using the STRING database and visualized with Cytoscape software (Figure 3A). Hub genes were

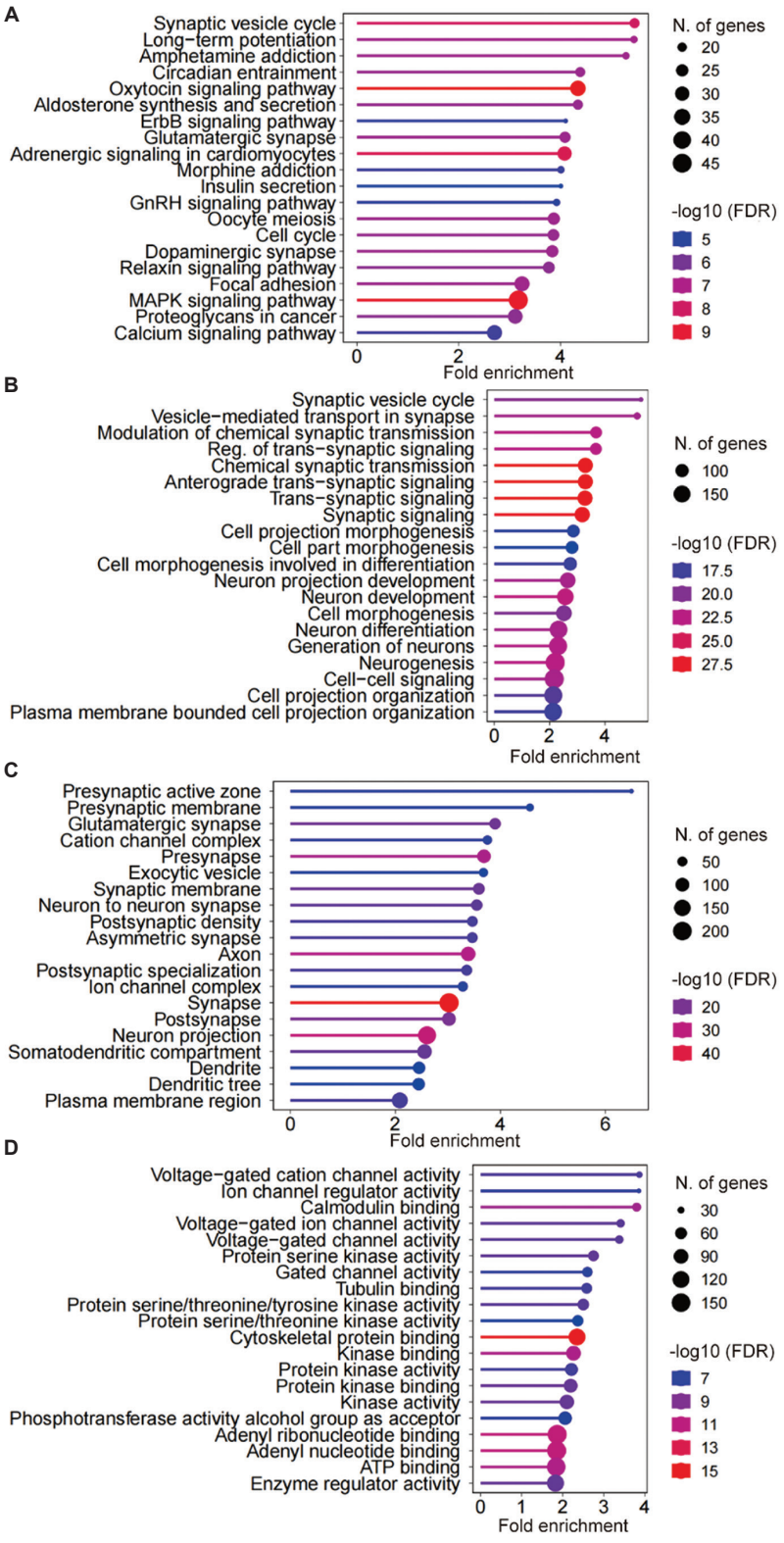

Figure 2. Enrichment analysis of overlapping differentially expressed genes. (A) KEGG pathway analysis. (B) Gene Ontology (GO) biological process enrichment analysis. (C) GO cellular component enrichment analysis. (D) GO MF enrichment analysis.

Abbreviations: ATP: Adenosine triphosphate; ErbB: Erythroblastic oncogene B; FDR: False discovery rate; GnRH: Gonadotropin-releasing hormone; MAPK: Mitogen-activated protein kinase.

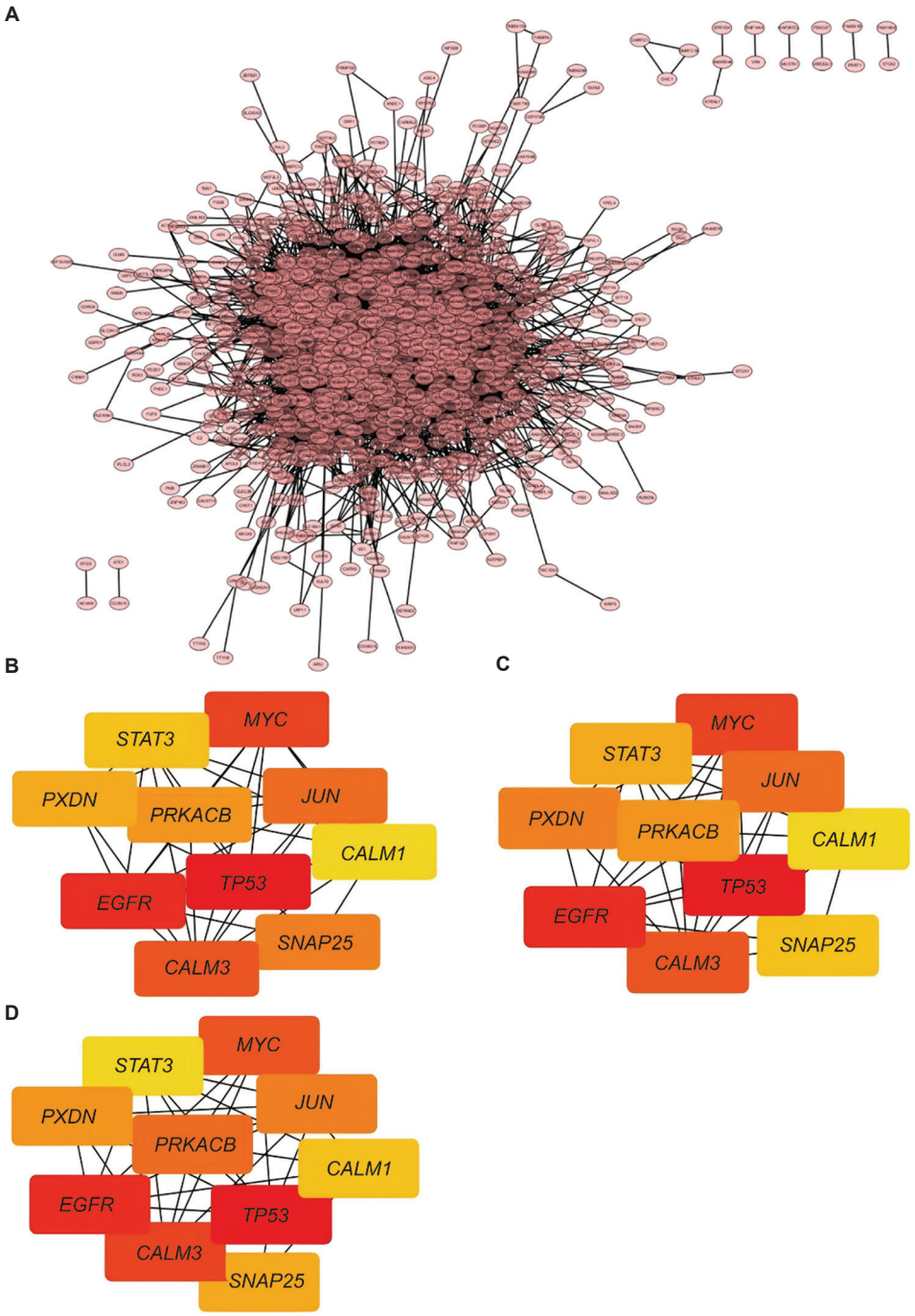

Figure 3. Identification of hub genes from the overlapping differentially expressed genes (DEGs) in two gene expression omnibus datasets. (A) Protein-protein interaction network of overlapping DEGs. Top 10 core genes identified using the (B) Closeness and (C) Radiality sorting methods. (D) Top 10 core genes identified using the Stress sorting method.
Abbreviations: CALM: Clathrin assembly lymphoid myeloid; EGFR: Epidermal growth factor receptor; PRKACB: Protein kinase CAMP-activated catalytic subunit beta; PXDN: Peroxidasin; SNAP25: Synaptosomal-associated protein, 25kDa; STAT3: Signal transducer and activator of transcription 3; TP53: Tumor protein p53.

identified using the CytoHubba plugin. Three sorting methods, namely closeness, radiality, and stress, were employed to determine the key genes. The top 10 core genes identified by each method are shown in Figure 3B-D. We found that the top 10 DEGs identified by all three algorithms were the same: *CALM1*, *CALM2*,

SNAP25, *CALM3*, *JUN*, *EGFR*, *PRKACB*, *PXDN*, *STAT3*, *TP53*, and *MYC*. To further validate the hub genes, we analyzed the expression levels of these 11 genes in both datasets. All but five genes (*CALM1*, *CALM2*, *STAT3*, *SNAP25*, and *PRKACB*) showed inconsistent expression changes between the two datasets, raising uncertainty about their roles in GBM development. Additional datasets are needed to verify their potential as marker genes (Figure 4A and B). Consistent expression changes across multiple GBM databases demonstrated the stability and importance of the five consistently expressed genes in disease progression. Therefore, these five genes (*CALM1*, *CALM2*, *STAT3*, SNAP25, and *PRKACB*) were selected for subsequent analysis.

3.4. Immune microenvironment in GBM and its association with hub gene expression and immune cell infiltration

Based on expression patterns in both datasets, *STAT3*, *CALM1*, *CALM2*, *SNAP25*, and *PRKACB* were determined as the final hub genes. To explore the immune microenvironment of GBM, the relative abundance of different immune cell subtypes was assessed based on the transcriptomes of all samples. The infiltration of immune cells in GBM patient tumor tissues and non-tumor tissues was evaluated. Figure 5A shows the percentages of different immune cell types in tumor and normal tissues in the GSE151352 dataset. By examining inflammatory cell infiltration, we explored the role of *STAT3*, *CAML1*, *CALM2*, *SNAP25*, and *PRKACB* in the GBM immune microenvironment. *STAT3* showed the strongest positive correlation with resting natural killer (NK) cells, while the other four genes exhibited negative correlations, as shown in Figure 5B. Similarly, in the GSE184643 dataset, Figure 6A depicts the relative abundance of different immune cell subgroups in the GBM background. Figure 6B shows the correlation analysis between immune cell infiltration and the expression levels of *STAT3*, *CALM1*, *CALM2*, *SNAP25*, and *PRKACB* in the GBM cohort. *STAT3* exhibited strong correlations with various immune cell types in the GBM background, most positively with B cells and most negatively with resting dendritic cells. *CALM1*, *CALM2*, *SNAP25*, and *PRKACB* were highly negatively correlated with plasma cells.

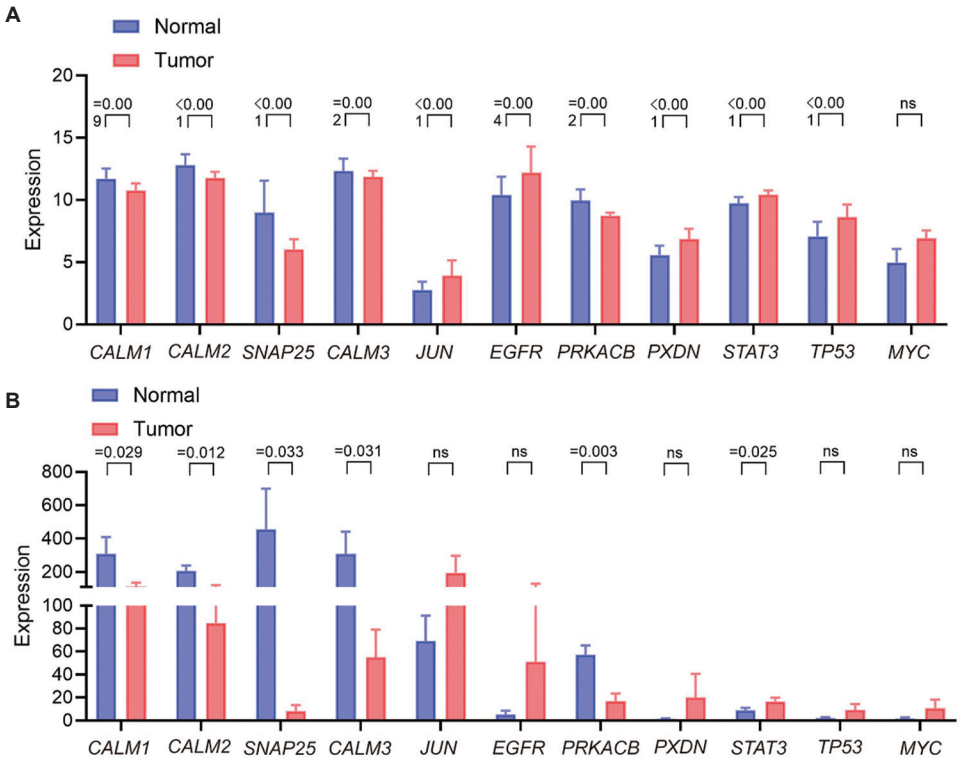

Figure 4. Expression patterns of the 10 core genes in two gene expression omnibus datasets. (A) Expression patterns of the 10 core genes in GSE151352. (B) Expression patterns of the 10 core genes in GSE184643.

Abbreviations: CALM: Clathrin assembly lymphoid myeloid; EGFR: Epidermal growth factor receptor; PRKACB: Protein kinase CAMP-activated catalytic subunit beta; PXDN: Peroxidasin; SNAP25: Synaptosomal-associated protein, 25kDa; STAT3: Signal transducer and activator of transcription 3; TP53: Tumor protein p53.

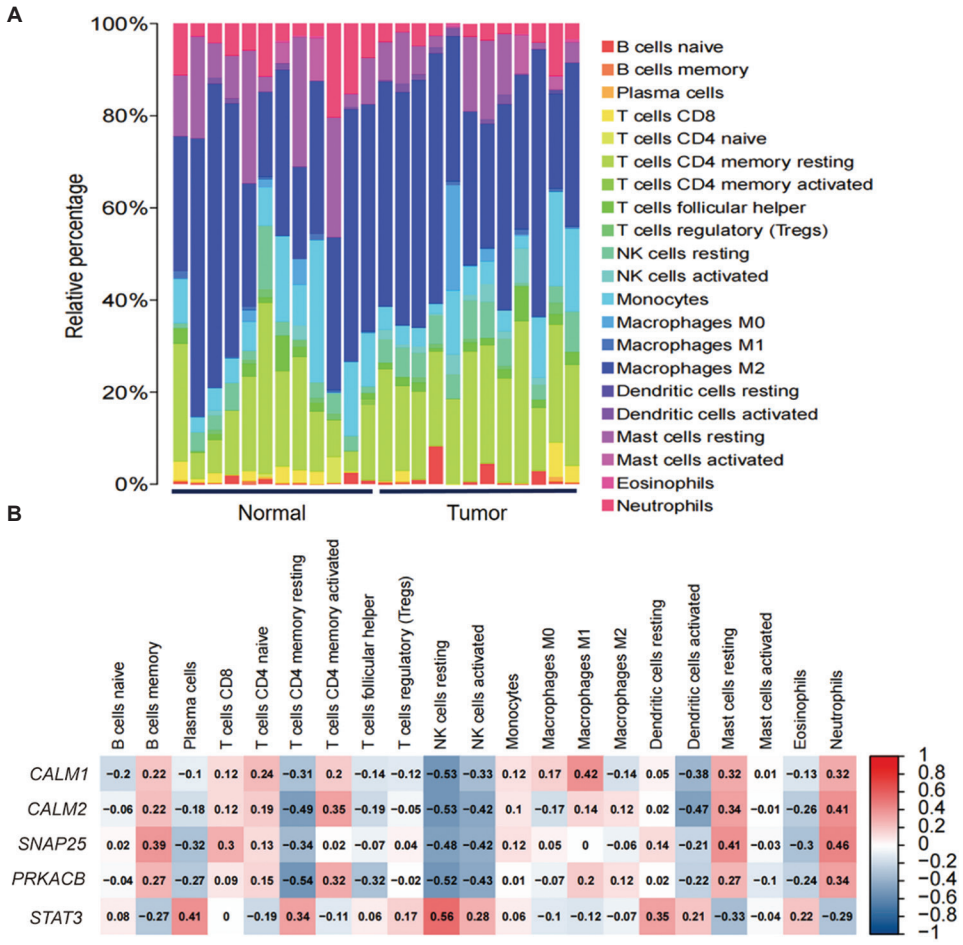

Figure 5. Immune infiltration in glioblastoma based on the GSE151352 dataset. (A) Percentages of various immune cells in normal and cancer tissues. (B) Correlation of the five hub genes with each immune cell type in the glioblastoma immune microenvironment, where red indicates a positive correlation, and blue indicates a negative correlation.
Abbreviations: CD: Cluster of differentiation; NK: Natural killer.

3.5. Diagnostic potential of *STAT3* and other hub genes for GBM evaluated by receiver operating curve analysis

Figure 7A-E displays the ROC curves and AUC statistics for *STAT3*, *CALM1*, *CALM2*, *SNAP25*, and *PRKACB* in the GSE151352 dataset. ROC curves were used to evaluate the performance of predictive models, and AUC reflects the overall accuracy of each model in distinguishing GBM cases from control samples. Among these genes, *STAT3* showed the highest diagnostic value, with an AUC of 0.8819. This finding provides valuable insights into the expression patterns of the core genes and highlights their potential as diagnostic markers for GBM.

3.6. PCR validation of *Stat3, Calm1, Calm2, Snap25,* and *Prkacb* mRNA expression in GBM tissues

This study conducted PCR experiments to verify the expression changes of hub genes between GBM and normal brain tissue samples. The results confirmed that GBM tissues exhibit an upregulation of *Stat3* mRNA levels compared to adjacent healthy tissues. In addition, *Calm1*, *Calm2*, *Snap25*, and *Prkacb* mRNA levels were downregulated in GBM tissues, consistent with the database findings (Figure 8).

3.7. Valproic acid as a potential therapeutic medicine targeting *STAT3, SNAP25, CALM1, CALM2,* and *PRKACB* in GBM

To explore potential anti-GBM therapeutics, we screened drugs targeting STAT3, SNAP25, CALM1, CALM2, and PRKACB using the DsigDB database. Table S1 lists the predicted chemical compounds with potential interactions with these five proteins. Among them, valproic acid emerged as a promising therapeutic agent for targeting STAT3, SNAP25, CALM1, CALM2, and PRKACB (Figure 9A). A binding affinity of ≤−5.0 kJ/mol is widely

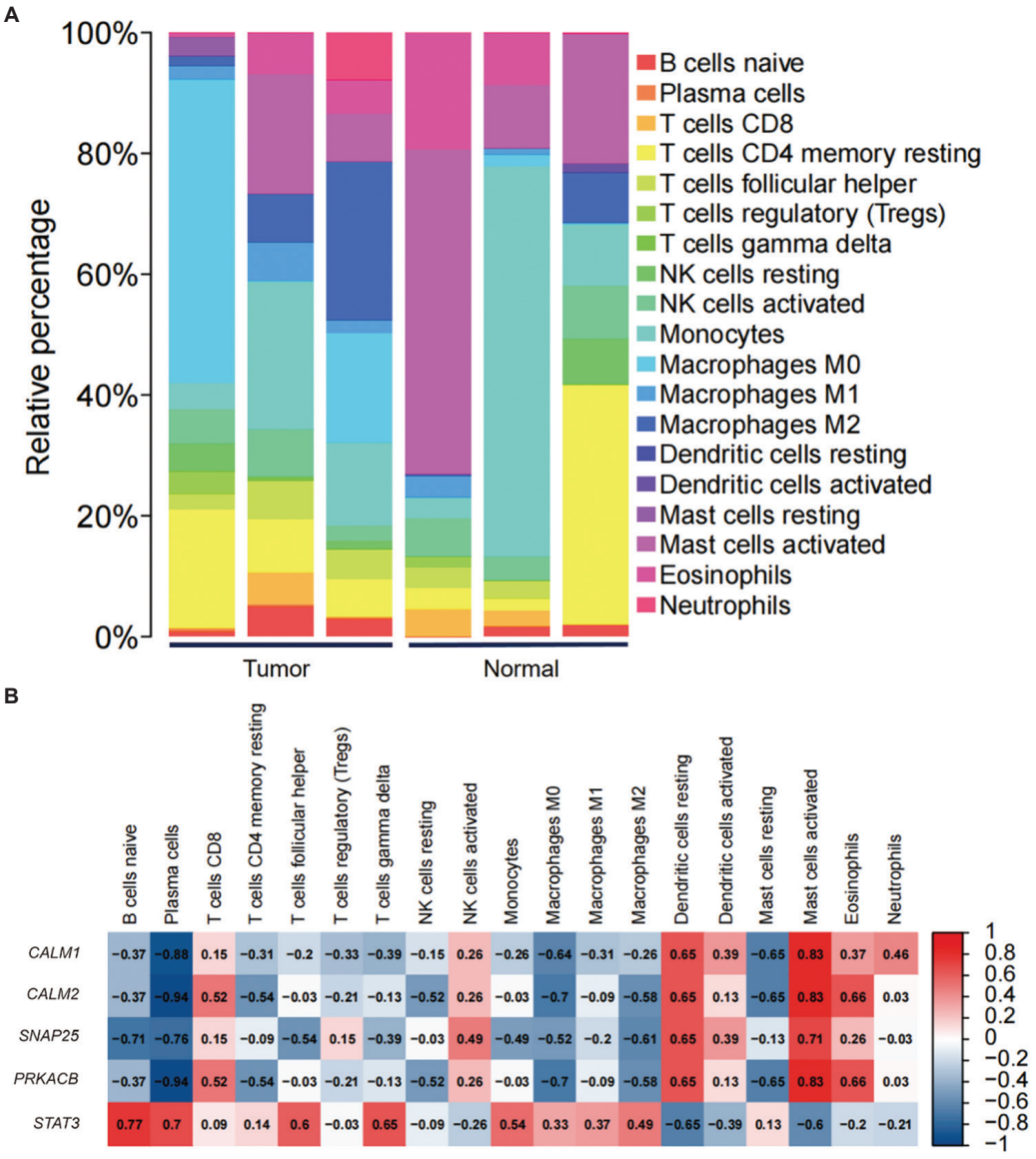

Figure 6. Immune infiltration in glioblastoma based on the GSE184643 dataset. (A) Percentages of various immune cells in normal and cancer tissues. (B) Correlation of the five hub genes with each immune cell type in the glioblastoma immune microenvironment, where red indicates a positive correlation, and blue indicates a negative correlation.
Abbreviations: CD: Cluster of differentiation; NK: Natural killer.

accepted as a benchmark in molecular docking, indicating stable and potentially physiologically relevant protein-ligand interactions.[38,39] Our findings show that valproic acid can bind to PRKACB, STAT3, and SNAP25 proteins. Among these, it exhibited the strongest binding affinity to PRKACB (−5.8 kJ/mol), followed by STAT3. The molecular docking results are illustrated in Figure 9B-F. For detailed binding information, refer to Table S2. These results suggest that valproic acid may exert a potential therapeutic effect on GBM through its interaction with these target proteins under the conditions of this study.

3.8. *In vitro* effects of valproic acid on STAT3, CALM, SNAP25, and PRKACB expression in GBM

To clarify the key pharmacological mechanism of valproic acid in treating GBM, as predicted by bioinformatics analysis, this study performed *in vitro* experiments to investigate its effects. LN229 and LN18 cell lines were utilized to assess valproic acid-induced GBM damage. The cells were exposed to varying doses of valproic acid, and cell viability was assessed using the CCK8 method. The results indicated a gradual decrease in cell survival rate with increasing concentrations of valproic acid in both

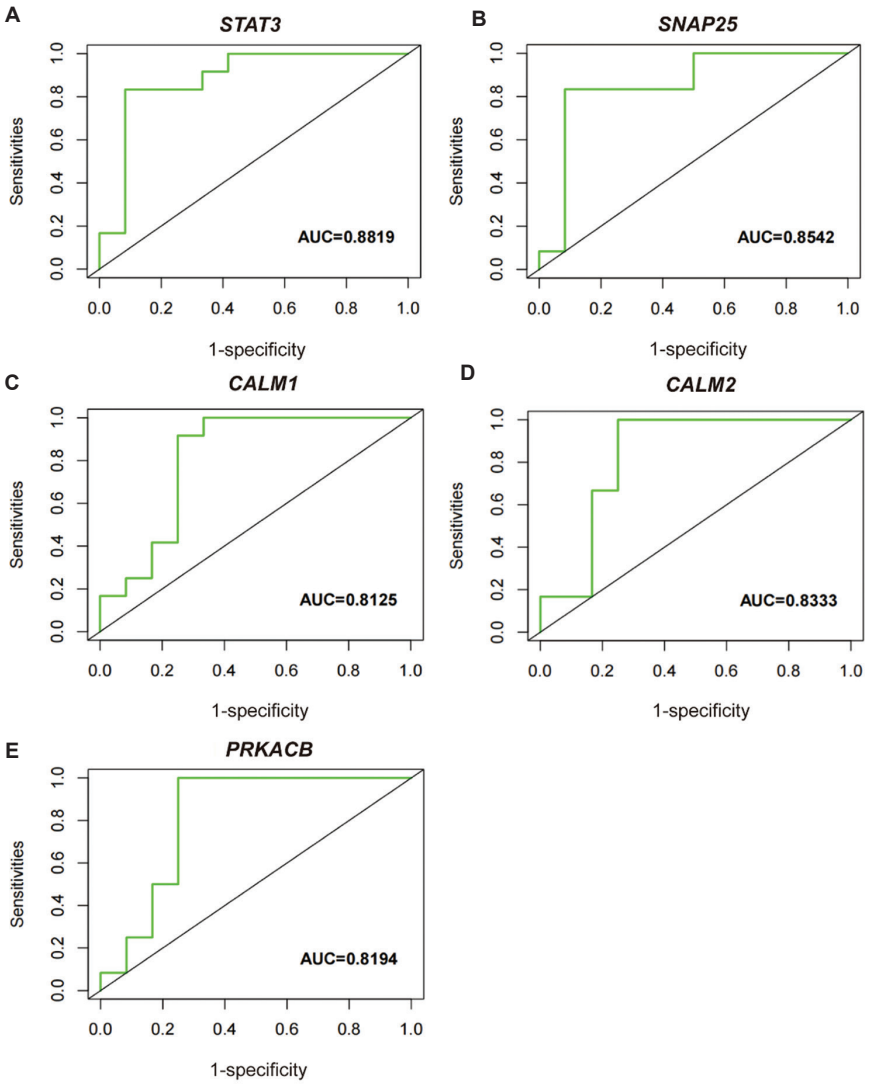

Figure 7. Diagnostic performance of the five hub genes. (A) *STAT3*; (B) *SNAP25*; (C) *CALM1*; (D) *CALM2*; (E) *PRKACB*.
Abbreviations: CALM: Clathrin assembly lymphoid myeloid; PRKACB: Protein kinase CAMP-activated catalytic subunit beta; SNAP25: Synaptosomal-associated protein, 25kDa; STAT3: Signal transducer and activator of transcription 3.

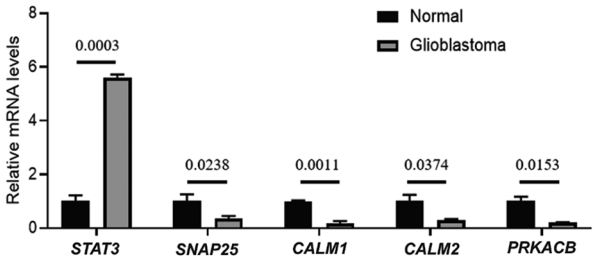

Figure 8. Differential messenger RNA (mRNA) expression levels of five hub genes in glioblastoma tissues compared to normal brain tissues of rats
Abbreviations: CALM: Clathrin assembly lymphoid myeloid; PRKACB: Protein kinase CAMP-activated catalytic subunit beta; SNAP25: Synaptosomal-associated protein, 25kDa; STAT3: Signal transducer and activator of transcription 3.

LN229 and LN18 cells (Figure 10A and B). Based on these results, the 10mM concentration group was selected for subsequent experiments. The relevant experimental findings demonstrated that valproic acid treatment significantly reduced the number of both types of cancer cells, suggesting a strong inhibitory effect on GBM cell growth (Figure 10C and D). In addition, comparative analysis showed that the migration ability of both cell lines was significantly reduced after treatment, indicating that valproic acid effectively inhibits both proliferation and migration of GBM cells (Figure 10E and F). To evaluate the expression changes of hub genes in cancer cells treated with valproic acid, Western blot analysis was conducted. The Western blot results showed that after valproic acid intervention, STAT3

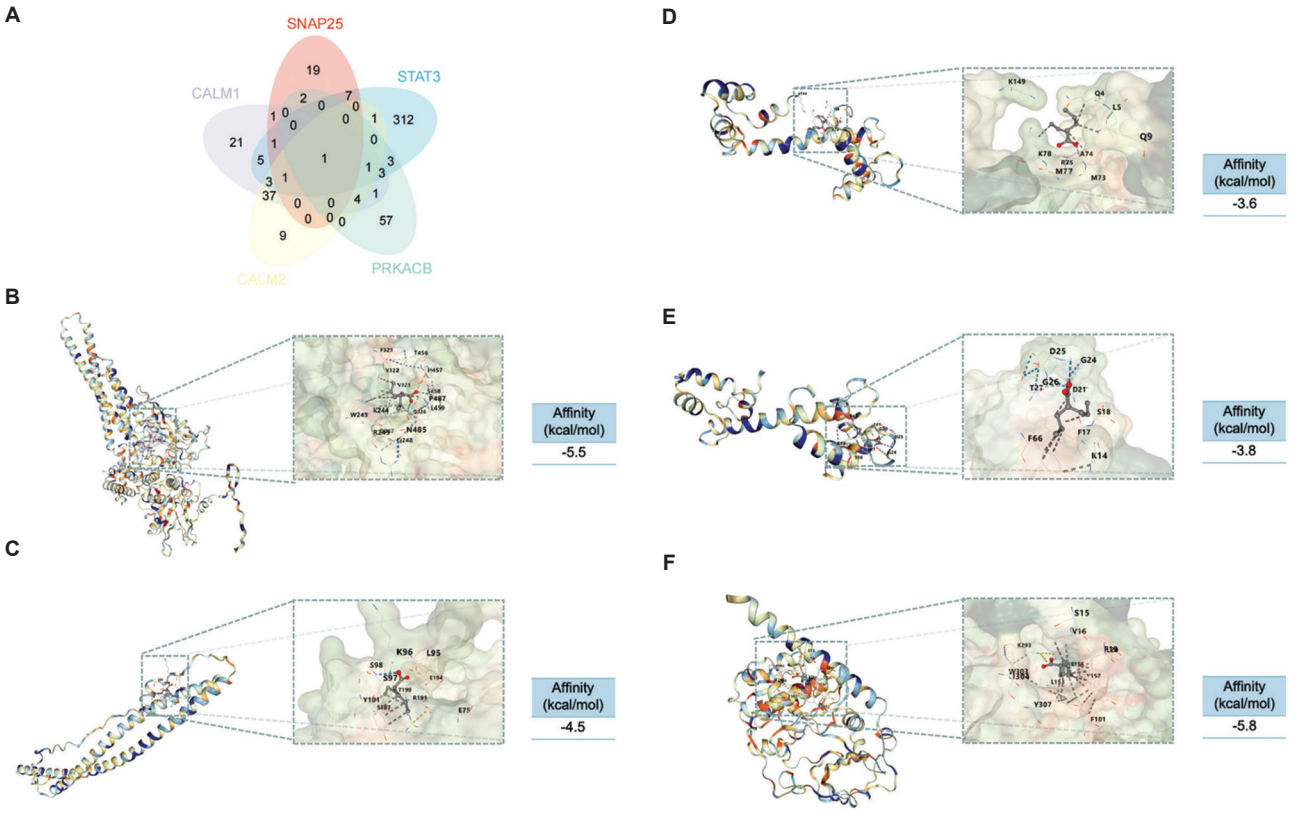

Figure 9. Identification of valproic acid as a potential therapeutic agent. (A) Venn diagram showing predicted intersections between chemical compounds with potential therapeutic effects on the five proteins. Five-dimensional molecular docking diagram of valproic acid with target proteins: (B) STAT3, (C) SNAP25, (D) CALM1, (E) CALM2, and (F) PRKACB.
Abbreviations: CALM: Clathrin assembly lymphoid myeloid; PRKACB: Protein kinase CAMP-activated catalytic subunit beta; SNAP25: Synaptosomal-associated protein, 25kDa; STAT3: Signal transducer and activator of transcription 3.

expression significantly decreased, while the expression levels of the other four core genes increased (Figure 10G and H). These results suggest that valproic acid may be used for targeted hub gene therapy in GBM.

4. Discussion

This study employed a series of methods to identify DEGs related to GBM and to clarify their roles in body tissues. In addition, the study analyzed the impact of pathological tissue on immune infiltration from different perspectives and drew corresponding conclusions. During this process, researchers conducted statistical and in-depth analyses of two independent datasets, resulting in a set of overlapping DEGs. Furthermore, functional enrichment analysis was performed on these DEGs. At the KEGG pathway analysis stage, the adrenergic pathway, cell cycle, and MAPK pathway in body tissues were significantly enriched. These findings suggest that these pathways are closely associated with GBM formation and may contribute to the disease's continued progression. The adrenergic signaling pathway mainly involves neurotransmitters related to adrenaline, which exert regulatory effects by activating specific receptors. This pathway regulates numerous important physiological processes and is closely tied to the body's adaptability to environmental changes, such as through the regulation of cell proliferation, migration, and angiogenesis. Research has found that abnormalities in the adrenergic pathway in GBM lead to increased proliferation and invasion of GBM cells, thereby promoting disease progression.[40] The MAPK pathway plays a crucial role in cell growth and differentiation, primarily by transmitting extracellular signals. In GBM, the MAPK pathway also exhibited significant abnormalities, resulting in increased tumor cell proliferation and reduced apoptosis. Abnormal activation of this pathway may also elevate the expression of related genes, thereby promoting angiogenesis and enhancing the immune evasion ability of cancer cells, ultimately accelerating GBM progression.[41] According to the enrichment analysis results, DEGs are mainly involved in synaptic transmission and intercellular communication, which can facilitate cancer cell metastasis and decrease drug sensitivity.[42] Therefore, changes in these processes may

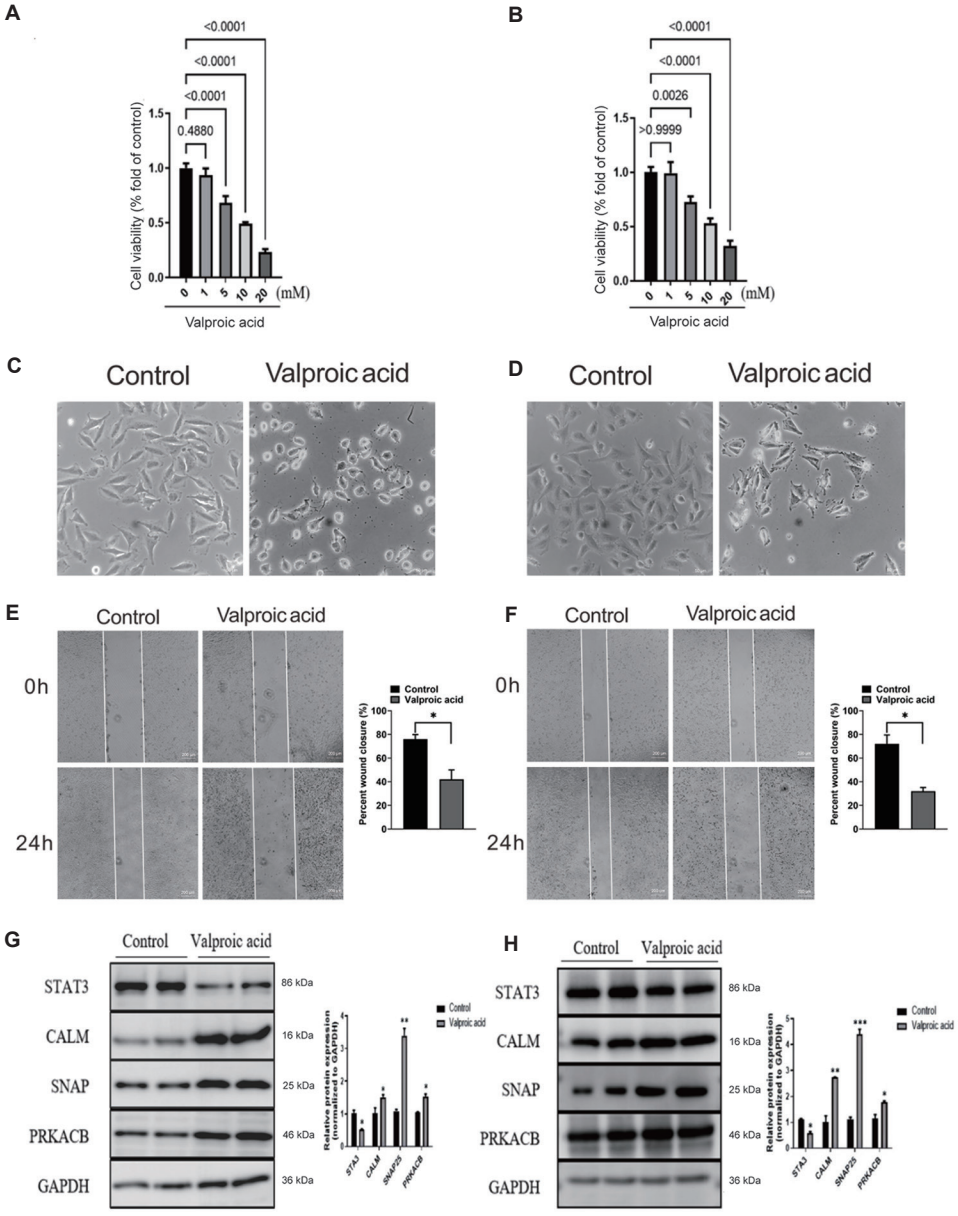

Figure 10. Valproic acid induces cytotoxicity in LN229 and LN18 cells and modulates hub gene expression patterns *in vitro*. (A) Cell viability of LN229 cells treated with different concentrations of valproic acid (1, 5, 10, and 20 mM) for 24 h (n = 3). (B) Cell viability of LN18 cells treated with different concentrations of valproic acid (1, 5, 10, and 20 mM) for 24 h (n = 3). (C) Effects of valproic acid on LN229 cell viability observed under optical microscopy (n = 3). Magnification = 40×; scale bar = 50 μm. (D) Effects of valproic acid on LN18 cell viability observed under optical microscopy (n = 3). Magnification = 40×; scale bar = 50 μm. (E) Effects of valproic acid on cell migration in LN229 cells (n = 3). Magnification = 10×; scale bar = 200 μm. (F) Effects of valproic acid on cell migration in LN18 cells (n = 3). Magnification = ×10; scale bar = 200 μm. (G) Representative Western blot images and quantitative analysis of STAT3, CALM, SNAP, and PRKACB expression in LN229 cells (n = 3). (H) Representative Western blot images and quantitative analysis of STAT3, CALM, SNAP, and PRKACB in LN18 cells (n = 3).

Abbreviations: CALM: Clathrin assembly lymphoid myeloid; GAPDH: glyceraldehyde 3-phosphate dehydrogenase; PRKACB: Protein kinase CAMP-activated catalytic subunit beta; SNAP25: Synaptosomal-associated protein, 25kDa; STAT3: Signal transducer and activator of transcription 3.

accelerate GBM progression and worsen patient prognosis. In the GO-CC category, the differentially expressed proteins were mainly related to neurons. These results support the view that GBM originates from glial cells in the brain. In addition, the analysis suggests that neuronal components play a significant role in the formation and spread of GBM.[43] Notably, GO-MF enrichment analysis revealed that DEGs in tissues not only significantly affect cytoskeletal protein binding but also influence various physiological activities such as kinase binding. Based on these findings, some

researchers speculate that these genes are closely related to cell signaling and play critical roles in the regulation of cytoskeletal structure and nucleotide metabolism. More importantly, these genes may be associated with the onset and progression of GBM, providing new avenues for the treatment of this disease.[44]

To identify core genes, PPI network analysis was conducted using the STRING database. Ten genes consistently identified as core genes were determined through three different ranking methods: *CALM1*, *CALM2*, *SNAP25*, *CALM3*, *JUN*, *EGFR*, *PRKACB*, *PXDN*, *STAT3*, *TP53*, and *MYC*. Subsequent expression analysis across the two datasets confirmed *STAT3*, *CALM1*, *CALM2*, SNAP25, and *PRKACB* as the final core genes. Notably, survival analysis revealed that high STAT3 expression significantly correlates with poor prognosis in GBM patients (Human Protein Atlas [HPA] database), aligning with our experimental findings and further supporting its therapeutic potential. However, while bioinformatics analysis indicated the downregulation of *CALM1* and *SNAP25* in GBM tissues, HPA data paradoxically associate their elevated expression with adverse outcomes. This discrepancy may arise from tissue-specific expression heterogeneity. HPA survival analyses are based on mixed cellular samples encompassing tumor microenvironment components (e.g., neurons, glia, and infiltrating immune cells), whereas our RNA-seq data specifically focus on tumor cells.[45] In addition, *CALM1* and *SNAP25* may exhibit tumor-suppressive roles during early GBM progression by maintaining calcium signaling homeostasis while potentially accelerating malignancy in later stages. Future studies will prospectively validate these findings through survival curve analyses using clinically annotated GBM samples. Furthermore, these DEGs were significantly enriched in multiple biological pathways and GO categories, suggesting important functional roles in GBM pathogenesis and progression. STAT3 is a key player in tumor-induced immunosuppression and is hyperactivated in both cancerous and non-cancerous cells within the tumor ecosystem. It inhibits the expression of immune activation regulators and promotes the production of immunosuppressive factors, thus impairing anti-tumor immune responses. In tumor cells, STAT3 decreases the expression of immune-stimulating cytokines, such as interferons, while increasing immunosuppressive cytokines and growth factors. This dual action contributes to an immunosuppressive tumor environment. *STAT3* also plays a role in immune cells, where its hyperactivation inhibits effective immune responses.[46] CALM1 and CALM2 are calmodulin-binding proteins involved in cellular signaling pathways. CALM1 contributes to synaptic plasticity and neurotransmitter release, which may indirectly influence immune cell function near the tumor site. CALM2, which is upregulated in certain cancers, may enhance malignancy and worsen prognosis by affecting cellular processes such as cell division and motility, potentially aiding tumor immune evasion.[47,48] Meanwhile, Janus kinase (JAK) plays a critical role in cytokine receptor signal transduction. Overexpression of CALM2 activates the JAK2/STAT3 signaling pathway, promoting macrophage polarization and thereby enhancing gastric cancer proliferation, migration, and invasion.[49] SNAP25 is a target SNARE protein critical for synaptic vesicle exocytosis in neurons. Although its role in the tumor microenvironment is less understood compared to STAT3, it is important for neuronal development and function. Given the interactions between the nervous and immune systems, alterations in SNAP25 expression or function may affect immune cell signaling and trafficking, though further studies are needed to elucidate these mechanisms.[50] PRKACB encodes the catalytic subunit of protein kinase A, which regulates cell proliferation and transcription. Its dysregulation can cause abnormal cell division, a hallmark of cancer. In the context of immune evasion, PRKACB may modulate the expression of genes involved in immune cell activity and the tumor microenvironment, though its precise mechanisms warrant further investigation.[51] Importantly, we analyzed the mRNA levels of hub genes in GBM tissues compared to normal brain tissues using PCR. The results revealed that several central genes exhibited significant expression changes, confirming the database analyses. These findings indicate that the identified genes are associated with GBM formation and may contribute to its progression. This study offers new insights into the molecular pathogenesis of GBM. Future research will employ tissue microarray technology in independent cohorts to validate protein co-localization, providing spatially resolved protein-level data critical for understanding tumor microenvironmental dynamics.

In addition to the above points, the study also focuses on a series of analyses exploring the correlation between GBM and immune infiltration. Comparative analysis revealed a significant difference in the proportion of immune cell types between the two groups of samples, indicating notable changes in the composition of immune cells within the tumor microenvironment. Statistical analysis also found a significant positive correlation between *STAT3* and resting NK cells, suggesting that this gene may regulate the level of inflammatory cell infiltration in GBM. The other four genes showed negative correlations with immune cell types, further demonstrating the significant association between *STAT3* and the proportion of immune cells in GBM. Research has found that STAT3 expression is positively correlated with the proportion of B cells,

which secrete various antibodies targeting antigens closely associated with cancer cells, thereby exerting relevant regulatory effects.[39] Except for *STAT3*, the other four genes were highly negatively correlated with plasma cells and positively correlated with activated mast cells. Comparative analysis showed that these results are consistent with previous studies. For example, some researchers have found that STAT3 plays a role in regulating immune responses and is closely related to tumor progression.[52] Under abnormal expression of CALM1, immune cell function is also significantly affected.[53] and this regulatory effect is mainly mediated through the calcium signaling pathway.[54] SNAP25 is closely related to immune cell activation and also influences inflammatory responses.[55,56] In terms of diagnosis, ROC curve results demonstrated that these five hub genes all have high diagnostic values, with STAT3 having the highest. Therefore, STAT3 has great potential in the diagnosis of GBM. Based on the molecular mechanism analysis in this study, we hypothesize that valproic acid exhibits therapeutic sensitivity primarily in specific GBM subtypes. First, in STAT3-driven GBM with high STAT3 expression, our findings demonstrate significant upregulation of STAT3 in GBM tissues, and valproic acid dose-dependently inhibits STAT3 expression. These results strongly suggest that STAT3-high GBM may represent a potential valproic acid-sensitive subtype. Second, KEGG pathway analysis revealed significant enrichment of DEGs in histone deacetylation-related pathways. Following valproic acid treatment, CALM1/2 expression levels were upregulated approximately twofold, indicating that valproic acid may ameliorate calcium signaling dysregulation by modulating the calmodulin network. Combined with previously reported histone deacetylase (HDAC) inhibitory effects, we propose that GBM subtypes with marked epigenetic abnormalities (e.g., whole-genome hypomethylation or specific histone modification patterns) may exhibit heightened sensitivity to valproic acid therapy.

This study also investigated potential anti-GBM drugs targeting these genes, providing support for the treatment of this disease. Valproic acid is a candidate drug for treating GBM, interacting with five core genes. Functioning as a multi-target epigenetic agent, VPA may exert synergistic anti-tumor effects by concurrently inhibiting STAT3 signaling and activating the CALM/SNAP25/PRKACB pathways. Valproic acid exhibits the characteristics of an HDAC inhibitor, which is of great significance for the treatment of GBM. This property can regulate the expression of related genes through epigenetic pathways, thereby promoting GBM cell apoptosis and inhibiting proliferation. However, the feasibility of using this drug to treat GBM is not yet fully clear.[57-59] After treatment with valproic acid, GBM patients may experience various side effects, such as nausea, vomiting, and gastrointestinal spasms, which also raise safety concerns. Liver injury is the most common complication, with a higher risk during the first 6 months of treatment. This issue is even more serious in infants and young children. Valproic acid can cause harm to the fetus, so pregnant women should use this medication with caution. The drug can also affect the pancreas and blood cells, leading to a range of side effects. Valproic acid has achieved significant results in clinical trials for GBM treatment and therefore, still shows broad application prospects. Some studies have combined it with temozolomide and found that it significantly improves overall survival and progression-free survival in patients. The drug also has a high ability to cross the blood-brain barrier, providing a significant advantage for treating GBM and enhancing efficacy. For epilepsy and psychiatric disorders, the long-term safety of valproic acid has been well established, indicating its potential feasibility in treating GBM.[60] Valproic acid has multiple effects on cell activity, mainly related to its HDAC inhibitor action. Through this action, silenced genes are activated, thereby regulating cell proliferation and apoptosis. Therefore, it can be used as an efficient epigenetic therapy agent to provide reliable support for the treatment of GBM. In addition, this drug can inhibit angiogenesis and suppress tumor cell proliferation and migration.[61] Molecular docking studies have shown that valproic acid exerts multiple effects as a drug targeting central genes. It has strong interactions with key genes, regulating pathways related to GBM progression. Targeted regulation of key proteins inhibits signals associated with tumor growth and invasion. This indicates that valproic acid, as a potential therapeutic drug for GBM, has strong molecular mechanism support. It inhibits the abnormal proliferation of cancer cells, which can hinder tumor progression and contribute to improving patient prognosis. Overall, these research results provide support for a deeper understanding of the mechanism of valproic acid treatment for GBM and offer guidance for relevant clinical trials. This study speculates that in combination therapy for this type of cancer, adding valproic acid as an adjunct drug can further enhance efficacy and improve prognosis. To gain a more comprehensive understanding of the therapeutic mechanism of this drug, we conducted a series of *in vitro* experiments using LN229 and LN18 cell lines. These cells are abundant in GBM. Further experimental research found that these two cell lines exhibit rapid growth, easy diffusion into surrounding normal tissues, and anti-apoptotic properties. To improve the reliability and robustness of the conclusions, multiple cell lines were used to obtain extensive data. When valproic acid was applied to GBM cells widely expressing the

aforementioned genes, the research team found that this drug acts in a concentration-dependent manner; in other words, the higher the drug concentration, the stronger the cytotoxic effect on LN229 and LN18 cells, resulting in a more effective therapeutic response. This suggests that valproic acid is feasible and effective for treating GBM. Further Western blot analysis showed that valproic acid can partially inhibit STAT3 synthesis in LN229 and LN18 cells while promoting the expression of CALM and SNAP. Overall, this drug effectively regulates hub gene expression, supporting its feasibility for cancer treatment. By downregulating STAT3, valproic acid may inhibit cell survival and proliferation, while the upregulation of CALM, SNAP, and PRKACB may contribute to the restoration of normal cellular processes disrupted in GBM.

However, there are certain limitations that need to be clarified. First, it is important to note that GBM is a heterogeneous disease with various molecular subtypes. Our study did not specifically investigate the differences in gene expression patterns among these subtypes. Future investigations should consider stratifying GBM patients based on their molecular characteristics to better understand the subtype-specific mechanisms underlying the disease. Second, while our findings point toward a role for these hub genes in GBM progression and treatment response, functional studies such as loss- and gain-of-function analyses are needed to elucidate their specific contributions. Such studies would provide insights into how these genes modulate tumor growth, invasion, and response to therapy. Finally, the molecular docking analysis identified valproic acid as a potential therapeutic candidate for GBM. However, it is important to note that molecular docking predictions do not guarantee actual binding or drug efficacy. *In vivo* experiments, including drug screening assays and preclinical studies, are necessary to evaluate the therapeutic potential of valproic acid and its mechanism of action in GBM. This study did not employ STAT3 inhibitors in the experimental validation; although preliminary findings demonstrated potential, their blood-brain barrier penetrability and toxicity profiles require further optimization. Future studies will combine valproic acid with STAT3 inhibitors in animal models or cellular assays to investigate valproic acid's regulatory effects on STAT3. In addition, the current cellular validation does not encompass all molecular subtypes. Subsequent research will expand to additional cellular subtypes (e.g., isocitrate dehydrogenase-mutant) to refine therapeutic strategies.

5. Conclusion

Our study identified overlapping DEGs associated with GBM and elucidated their potential functional roles through comprehensive bioinformatics analyses. We identified hub genes, including *STAT3*, *CALM1*, *CALM2*, *SNAP25*, and *PRKACB*, which exhibited consistent differential expression patterns and demonstrated diagnostic and therapeutic potential. In addition, we found that valproic acid could potentially exert therapeutic effects on GBM. Further experimental validations and functional studies are warranted to confirm these findings and explore the underlying mechanisms of these genes in GBM pathogenesis and immune responses.

Acknowledgments

None.

Funding

None.

Conflict of interest

The authors declare no conflicts of interest.

Author contributions

Conceptualization: Leina Li
Data curation: Moli Wu, Xu Zheng
Formal analysis: Xu Zheng
Investigation: Leina Li
Methodology: Moli Wu
Writing – original draft: Leina Li
Writing – review & editing: Jia Liu

Ethics approval and consent to participate

All animal experiments complied with the ARRIVE (Animal Research: Reporting of *in vivo* Experiments) guidelines and were performed in accordance with the National Institutes of Health Guide for the Care and Use of Laboratory Animals. The experiments were approved by the Laboratory Animal Welfare and Ethics Committee of Dalian Medical University (Approval No. AEE23014).

Consent for publication

Not applicable.

Availability of data

Data are available from the corresponding author upon request.

References

1. Rayati M, Mansouri V, Ahmadbeigi N. Gene therapy in glioblastoma multiforme: Can it be a role changer? *Heliyon*. 2024;10(5):e27087.

   doi: 10.1016/j.heliyon.2024.e27087

2. Hamad A, Yusubalieva GM, Baklaushev VP, Chumakov PM,

Lipatova AV. Recent developments in glioblastoma therapy: Oncolytic viruses and emerging future strategies. *Viruses*. 2023;15(2):547.

doi: 10.3390/v15020547

3. Minniti G, Niyazi M, Alongi F, Navarria P, Belka C. Current status and recent advances in reirradiation of glioblastoma. *Radiat Oncol*. 2021;16(1):36.

doi: 10.1186/s13014-021-01767-9

4. Perry JR, Laperriere N, O'Callaghan CJ, *et al*. Short-course radiation plus temozolomide in elderly patients with glioblastoma. *N Engl J Med*. 2017;376(11):1027-1037.

doi: 10.1056/NEJMoa1611977

5. Ye L, Gu L, Wang Y, *et al*. Identification of TMZ resistance-associated histone post-translational modifications in glioblastoma using multi-omics data. *CNS Neurosci Ther*. 2024;30(3):e14649.

doi: 10.1111/cns.14649

6. Li K, Du Y, Li L, Wei DQ. Bioinformatics approaches for anti-cancer drug discovery. *Curr Drug Targets*. 2020;21(1):3-17.

doi: 10.2174/1389450120666190923162203

7. Tran TO, Vo TH, Lam LHT, Le NQK. ALDH2 as a potential stem cell-related biomarker in lung adenocarcinoma: Comprehensive multi-omics analysis. *Comput Struct Biotechnol J*. 2023;21:1921-1929.

doi: 10.1016/j.csbj.2023.02.045

8. Dang HH, Ta HDK, Nguyen TTT, *et al*. Identifying GPSM family members as potential biomarkers in breast cancer: A comprehensive bioinformatics analysis. *Biomedicines*. 2021;9(9):1144.

doi: 10.3390/biomedicines9091144

9. Cakir MU, Yavuz-Aksu B, Aksu U. Hypervolemia suppresses dilutional anaemic injury in a rat model of haemodilution. *J Transl Int Med*. 2022;11(4):393-400.

doi: 10.2478/jtim-2022-0045

10. Chen X, Wang M, Yu K, *et al*. Chronic stress-induced immune dysregulation in breast cancer: Implications of psychosocial factors. *J Transl Int Med*. 2022;11(3):226-233.

doi: 10.2478/jtim-2021-0050

11. Deng M, Wang M, Zhang Q, *et al*. Point-of-care ultrasound-guided submucosal paclitaxel injection in tracheal stenosis model. *J Transl Int Med*. 2023;11(1):70-80.

doi: 10.2478/jtim-2022-0044

12. Deng Y, Wang H, Guo X, Jiang S, Cai J. Long-term blood pressure outcomes of laparoscopic adrenalectomy in trHTN patients. *J Transl Int Med*. 2021;11(1):275-281.

doi: 10.2478/jtim-2023-0107

13. Kanehisa M, Furumichi M, Sato Y, Ishiguro-Watanabe M, Tanabe M. KEGG: Integrating viruses and cellular organisms. *Nucleic Acids Res*. 2021;49(D1):D545-D551.

doi: 10.1093/nar/gkaa970

14. Dennis G Jr., Sherman BT, Hosack DA, *et al*. DAVID: Database for annotation, visualization, and integrated discovery. *Genome Biol*. 2003;4(5):P3.

15. Dou L, Lu E, Tian D, Li F, Deng L, Zhang Y. Adrenomedullin induces cisplatin chemoresistance in ovarian cancer through reprogramming of glucose metabolism. *J Transl Int Med*. 2023;11(2):169-177.

doi: 10.2478/jtim-2023-0091

16. Cao Y, Lan W, Wen L, *et al*. An effectiveness study of a wearable device (Clouclip) intervention in unhealthy visual behaviors among school-age children: A pilot study. *Medicine (Baltimore)*. 2020;99(2):e17992.

doi: 10.1097/MD.0000000000017992

17. Chen L, Tian Q, Shi Z, Qiu Y, Lu Q, Liu C. Melatonin alleviates cardiac function in sepsis-caused myocarditis via maintenance of mitochondrial function. *Front Nutr*. 2021;8:754235.

doi: 10.3389/fnut.2021.754235

18. Rigopoulou I, Bakarozi E, Dimas M, *et al*. Total and individual PBC-40 scores are reliable for the assessment of health-related quality of life in Greek patients with primary biliary cholangitis. *J Transl Int Med*. 2023;11(3):246-254.

doi: 10.2478/jtim-2023-0098

19. Chen L, Zhan CZ, Wang T, You H, Yao R. Curcumin inhibits the proliferation, migration, invasion, and apoptosis of diffuse large B-cell lymphoma cell line by regulating MiR-21/VHL axis. *Yonsei Med J*. 2020;61(1):20-29.

doi: 10.3349/ymj.2020.61.1.20

20. He Q, Li J. The evolution of folate supplementation - from one size for all to personalized, precision, poly-paths. *J Transl Int Med*. 2023;11(2):128-137.

doi: 10.2478/jtim-2023-0087

21. Cuny H, Bozon K, Kirk RB, Sheng DZ, Bröer S, Dunwoodie SL. Maternal heterozygosity of Slc6a19 causes metabolic perturbation and congenital NAD deficiency disorder in mice. *Dis Model Mech*. 2023;16(5):dmm049647.

doi: 10.1242/dmm.049647

22. Hyug Choi J, Sook Jun M, Yong Jeon J, *et al*. Global lineage evolution pattern of SARS-COV-2 in Africa, America, Europe, and Asia: A comparative analysis of variant clusters and their relevance across continents. *J Transl Int Med*. 2023;11(4):410-422.

doi: 10.2478/jtim-2023-0118

23. Yoo M, Shin J, Kim J, *et al*. DSigDB: Drug signatures database for gene set analysis. *Bioinformatics*. 2015;31(18):3069-3071.

doi: 10.1093/bioinformatics/btv313

24. Li Y, Yao Z, Li Y, *et al*. Prognostic value of serum ammonia in critical patients with non-hepatic disease: A prospective, observational, multicenter study. *J Transl Int Med*. 2022;11(4):401-409.

doi: 10.2478/jtim-2022-0021

25. Eberhardt J, Santos-Martins D, Tillack AF, Forli S. AutoDock vina 1.2.0: New docking methods, expanded force field, and python bindings. *J Chem Inf Model*. 2021;61(8):3891-3898.

doi: 10.1021/acs.jcim.1c00203

26. Ding L, Lu S, Zhou Y, *et al*. The 3' untranslated region protects the heart from angiotensin ii-induced cardiac dysfunction via AGGF1 expression. *Mol Ther*. 2020;28(4):1119-1132.

doi: 10.1016/j.ymthe.2020.02.002

27. Gao WL, Li XH, Dun XP, Jing XK, Yang K, Li YK. Grape seed proanthocyanidin extract ameliorates streptozotocin-induced cognitive and synaptic plasticity deficits by inhibiting oxidative stress and preserving AKT and ERK activities. *Curr Med Sci*. 2020;40(3):434-443.

doi: 10.1007/s11596-020-2197-x

28. Liu N, Li D, Liu D, Liu Y, Lei J. FOSL2 participates in renal fibrosis via SGK1-mediated epithelial-mesenchymal transition of proximal tubular epithelial cells. *J Transl Int Med*. 2023;11(3):294-308.

doi: 10.2478/jtim-2023-0105

29. Song X, Shu XH, Wu ML, *et al*. Postoperative resveratrol administration improves prognosis of rat orthotopic glioblastomas. *BMC Cancer*. 2018;18:871.

doi: 10.1186/s12885-018-4771-1

30. Xue S, Xiao-Hong S, Lin S, *et al*. Lumbar puncture-administered resveratrol inhibits STAT3 activation, enhancing autophagy and apoptosis in orthotopic rat glioblastomas. *Oncotarget*. 2016;7(46):75790-75799.

doi: 10.18632/oncotarget.12414

31. Huang Z, Yu P, Tang J. Characterization of triple-negative breast cancer MDA-MB-231 cell spheroid model. *Onco Targets Ther*. 2020;13:5395-5405.

doi: 10.2147/OTT.S249756

32. Liu Y, Liu Y, Ye S, Feng H, Ma L. A new ferroptosis-related signature model including messenger RNAs and long non-coding RNAs predicts the prognosis of gastric cancer patients. *J Transl Int Med*. 2023;11(2):145-155.

doi: 10.2478/jtim-2023-0089

33. Jiang L, Chen T, Xiong L, *et al*. Knockdown of m6A methyltransferase METTL3 in gastric cancer cells results in suppression of cell proliferation. *Oncol Lett*. 2020;20(3):2191-2198.

doi: 10.3892/ol.2020.11794

34. Lu Y, Lin Z, Wen L, *et al*. The adaptation and acceptance of defocus incorporated multiple segment lens for Chinese children. *Am J Ophthalmol*. 2020;211:207-216.

doi: 10.1016/j.ajo.2019.12.002

35. Peng Y, Wang Y, Zhou C, Mei W, Zeng C. PI3K/Akt/mTOR pathway and its role in cancer therapeutics: Are we making headway? *Front Oncol*. 2022;12:819128.

doi: 10.3389/fonc.2022.819128

36. Wen L, Cao Y, Cheng Q, *et al*. Objectively measured near work, outdoor exposure and myopia in children. *Br J Ophthalmo*l. 2020;104(11):1542-1547.

doi: 10.1136/bjophthalmol-2019-315258

37. Yu W, Qin X, Zhang Y, *et al*. Curcumin suppresses doxorubicin-induced cardiomyocyte pyroptosis via a PI3K/Akt/mTOR-dependent manner. *Cardiovasc Diagn Ther*. 2020;10(4):752-769.

doi: 10.21037/cdt-19-707

38. Xu P, Fu G, Zhao H, *et al*. Review of molecular biological research on the treatment of membranous nephropathy with *Tripterygium* glycosides based on TCM theory. *Medicine (Baltimore)*. 2023;102(45):e34686.

doi: 10.1097/MD.0000000000034686

39. Yang Z, Li J, Song H, *et al*. Unraveling the molecular links between benzopyrene exposure, NASH, and HCC: An integrated bioinformatics and experimental study. *Sci Rep*. 2023;13(1):20520.

doi: 10.1038/s41598-023-46440-1

40. Kraboth Z, Kalman B. ß-Adrenoreceptors in human cancers. *Int J Mol Sci*. 2023;24(4):3671.

doi: 10.3390/ijms24043671

41. Wong SC, Kamarudin MNA, Naidu R. Anticancer mechanism of curcumin on human glioblastoma. *Nutrients*. 2021;13(3):950.

doi: 10.3390/nu13030950

42. Maacha S, Bhat AA, Jimenez L, *et al*. Extracellular vesicles-mediated intercellular communication: Roles in the tumor microenvironment and anti-cancer drug resistance. *Mol Cancer*. 2019;18(1):55.

doi: 10.1186/s12943-019-0965-7

43. Kim HJ, Park JW, Lee JH. Genetic architectures and cell-of-origin in glioblastoma. *Front Oncol*. 2021;10:615400.

doi: 10.3389/fonc.2020.615400

44. Ahir BK, Engelhard HH, Lakka SS. Tumor development and angiogenesis in adult brain tumor: Glioblastoma. *Mol Neurobiol*. 2020;57(5):2461-2478.

doi: 10.1007/s12035-020-01892-8

45. Zhang C, Wang X, Li X, *et al*. Targeting the IGF2BP3-

SEMA3A axis inhibits angiogenesis in glioblastoma. *J Clin Invest*. 2022;132(10):e154536.

46. Fu W, Hou X, Dong L, Hou W. Roles of STAT3 in the pathogenesis and treatment of glioblastoma. *Front Cell Dev Biol*. 2023; 11: 1098482. doi:10.3389/fcell.2023.1098482

47. Sung H, Hyland PL, Pemov A, *et al*. Genome-wide association study of café-au-lait macule number in neurofibromatosis type 1. *Mol Genet Genomic Med*. 2020;8(10):e1400.

doi: 10.1002/mgg3.1400

48. Garg A, Pal D. Exploring the use of molecular dynamics in assessing protein variants for phenotypic alterations. *Hum Mutat*. 2019;40(9):1424-1435.

doi: 10.1002/humu.23800

49. Wang Y, Jiang Y, Zhang M, *et al*. Regulation of SEMA3G by IGF2BP3 promotes glioblastoma progression through PI3K-AKT signaling. *Neuro Oncol*. 2021;23(12):2089-2102.

50. Huang Q, Lian C, Dong Y, *et al*. SNAP25 inhibits glioma progression by regulating synapse plasticity via GLS-mediated glutaminolysis. *Front Oncol*. 2021;11:698835.

doi: 10.3389/fonc.2021.698835

51. Jiang K, Yao G, Hu L, *et al*. MOB2 suppresses GBM cell migration and invasion via regulation of FAK/Akt and cAMP/PKA signaling. *Cell Death Dis*. 2020;11(4):230.

doi: 10.1038/s41419-020-2381-8

52. Tsai CH, Chuang YM, Li X, *et al*. Immunoediting instructs tumor metabolic reprogramming to support immune evasion. *Cell Metab*. 2023;35(1):118-133.e7.

doi: 10.1016/j.cmet.2022.12.003

53. Yao M, Fu L, Liu X, Zheng D. *In-silico* multi-omics analysis of the functional significance of calmodulin 1 in multiple cancers. *Front Genet*. 2022;12:793508.

doi: 10.3389/fgene.2021.793508

54. Colomer J, Agell N, Engel P, Bachs O. Expression of calmodulin and calmodulin binding proteins in lymphoblastoid cells. *J Cell Physiol*. 1994;159(3):542-550.

doi: 10.1002/jcp.1041590318

55. Di L, Gu M, Wu Y, *et al*. SNAP25 is a potential prognostic biomarker for prostate cancer. *Cancer Cell Int*. 2022;22(1):144.

doi: 10.1186/s12935-022-02558-2

56. Moen LV, Sener Z, Volchenkov R, *et al*. Ablation of the Cβ2 subunit of PKA in immune cells leads to increased susceptibility to systemic inflammation in mice. *Eur J Immunol*. 2017;47(11):1880-1889.

doi: 10.1002/eji.201646809

57. Franco-Juárez EX, González-Villasana V, Camacho-Moll ME, *et al*. Mechanistic insights about sorafenib-, valproic acid- and metformin-induced cell death in hepatocellular carcinoma. *Int J Mol Sci*. 2024; 25(3):1760.

doi: 10.3390/ijms25031760

58. Cai Z, Lim D, Liu G, *et al*. Valproic acid-like compounds enhance and prolong the radiotherapy effect on breast cancer by activating and maintaining anti-tumor immune function. *Front Immunol*. 2021;12:646384.

doi: 10.3389/fimmu.2021.646384

59. Duenas-Gonzalez A, Candelaria M, Perez-Plascencia C, Perez-Cardenas E, de la Cruz-Hernandez E, Herrera LA. Valproic acid as epigenetic cancer drug: Preclinical, clinical and transcriptional effects on solid tumors. *Cancer Treat Rev*. 2008;34(3):206-222.

doi: 10.1016/j.ctrv.2007.11.003

60. Tsai HC, Wei KC, Chen PY, *et al*. Valproic acid enhanced temozolomide-induced anticancer activity in human glioma through the p53-PUMA apoptosis pathway. *Front Oncol*. 2021;11:722754.

doi: 10.3389/fonc.2021.722754

61. Sun J, Piao J, Li N, Yang Y, Kim KY, Lin Z. Valproic acid targets HDAC1/2 and HDAC1/PTEN/Akt signalling to inhibit cell proliferation via the induction of autophagy in gastric cancer. *FEBS J*. 2020;287(10):2118-2133.

doi: 10.1111/febs.15122